Electronics and Electrical Engineering

AIMS Electronics and Electrical Engineering, 9(4): 476–499.
DOI: 10.3934/electreng.2025022
Received: 19 May 2025
Revised: 11 August 2025
Accepted: 25 August 2025
Published: 02 September 2025

https://www.aimspress.com/journal/ElectrEng

Research article

Performance assessment of a solar PV array using a new dynamic reconfiguration based on the Cuckoo Search optimizer

Hassan S. Ahmed[1], Ahmed J. Abid[2], Adel A. Obed[2], Raaid Alubady[3,4], Salam J. Yaqoob[5], Ameer L. Saleh[6,*] and László Számel[6]

[1] Technology Department: Medical Device Engineering, Al-Farahidi University, Baghdad 10001, Iraq
[2] Department of Electrical Power Engineering, Middle Technical University, Baghdad 10001, Iraq
[3] Department of Computer Techniques Engineering, Engineering Technical College, Al-Ayen University, Thi-Qar, Iraq
[4] Department of Information Networks, College of Information Technology, University of Babylon, Babel, Iraq
[5] Training and Energy Researches Office, Ministry of Electricity, Baghdad 10001, Iraq
[6] Budapest University of Technology and Economics, Department of Electric Power Engineering, H-1111 Budapest, Hungary

*** Correspondence:** Email: aalkalmashi@edu.bme.hu.

Abstract: Partial shading is a major challenge in photovoltaic (PV) systems, as it causes significant power losses and leads to multiple local maximum power points (MPPs) on the power-voltage (P-V) curve, reducing overall system efficiency. To address this issue, we proposed a novel reconfiguration approach for shaded PV arrays using the Cuckoo Search (CS) optimization algorithm. With the proposed method, we aimed to identify an optimal switching matrix structure that minimizes current mismatch among rows and maximizes power output under shading conditions. The methodology involved implementing a 9×9 PV array model in MATLAB/Simulink and evaluating its performance under five distinct shading patterns. The performance of the CS-based reconfiguration was compared against four established techniques: Total Cross-Tied (TCT), standard Sudoku, Optimal Sudoku, and the Multi-objective Grey Wolf Optimizer (MOGWO). The evaluation was based on key statistical and performance metrics, including on power output, system reliability, and convergence behavior. Testing results demonstrated the superiority of the CS method, achieving global maximum power point (GMPP) values of 23.6071 kW, 23.0057 kW, 22.1083 kW, 22.6669 kW, and 22.4937 kW across the five tested shading scenarios. These results validated the effectiveness of

the CS algorithm in enhancing the power output of PV arrays under partial shading and highlight its potential applicability in real-world energy systems.

Keywords: Cuckoo Search optimizer; PV; PV reconfiguration; PV interconnection schemes; partial shading mitigation

1. Introduction

Most power is generated using conventional energy sources such as coal, oil, and natural gas. These sources emit carbon dioxide, which contributes to the issue of global warming. The direct cause of climate change is the burning of fossil fuels, which emit greenhouse gases (GHG) into the atmosphere. Nearly 80% of GHGs are caused by the use of fossil fuels. Regardless, the world's primary energy demand is projected to expand by nearly 60% between 2002 and 2030, with an average annual growth of 1.7%, leading to other GHG emissions. Oil reserves are projected to be exhausted by 2040, natural gas by 2060, and coal by 2300 [1]. Considering the current situation, there is a growing need to develop renewable energy sources (RES) to create clean and emission-free energy. The search for RES has evolved into an urgent issue [2,3]. RES such as wind power, fuel cells (FC), and photovoltaic (PV) are increasingly being employed more frequently in different applications, including motor drives, uninterruptible power systems, electric vehicles, microgrids, and more. Solar energy is the most critical and sustainable resource due to its ubiquity and quantity in nature. Besides requiring little maintenance, it is fuel-free and pollution-free. The output power of PV relies on the number of connected PV modules and their structure, as well as the local environmental situations [4–6]. The current worldwide instantaneous evolution of PV systems has significantly accelerated research efforts toward improving efficiency, reliability, and large-scale integration into modern power grids [7]. Furthermore, the immediate integration of PV systems into electrical networks has created gaps for further development of more capable energy management systems. One of the most critical challenges within the operation of PV arrays is the occurrence of partial shading mismatch losses, which reduce energy yield and are highly problematic. Conventional fixed configurations suffer from a stagnant response to shifting environmental conditions, leading to underperformance. Dynamic reconfiguration solves these issues of mismatch loss and energy generation by making real-time adjustments to the electrical connections in the PV modules. Yet, determining the optimal pattern in dynamic reconfiguration is a complex combinatorial problem that requires sophisticated optimization techniques. Moreover, the PV array connects many PV panels in series/parallel or both.

Various interconnection techniques that are known to create a PV array are (i) Series-Parallel (SP), (ii) Bridged-Link (BL), (iii) Honey-Comb (HC), and (iv) Total Cross Tied (TCT) methods. Moreover, the most typically utilized interconnection strategy for output power enhancement with a significant decrease in mismatch power losses under partial shading conditions (PSC) is the TCT arrangement [8]. Moreover, the PSC is the most significant issue affecting PV efficiency. The PSC occurs if the PV modules are shaded in the PV array cause of flying birds, passing clouds, and adjacent buildings. Under PSCs, the quantity of irradiance obtained by the shaded module is less than that obtained by the unshaded module [6]. The alternative solution proposed for handling the PSC phenomenon's harmful impact is rearranging the shaded modules in the array; this process is described as a reconfiguration of the PV array. The main target of the PV array reconfiguration strategy is to

minimize power loss and improve the global maximum power (GMP). Different array reconfiguration approaches that are employed in practice can be organized into: Physical relocation [9,10], Electrical rewiring [11,12], and Electrical Array Reconfiguration methods (EAR) [13,14]. The EAR has emerged as an alternative strategy in the PV array reconfiguration domain, where shade distribution can be performed via the switch matrix with dimension (m × n). Moreover, this approach is called dynamic re-configuration [15].

Numerous researchers suggested various topologies of the shaded PV array either via static or dynamic reconfiguration approach; some of the reported works are examined as follows: The genetic algorithm, GA, was employed for reconfiguration to improve the energy output of a TCT-connected shade PV system [16]. Babu. et al. [17] recommended using particle swarm optimization (PSO) to reposition shaded PV modules for increased power output. The authors in [18] proposed a Sudoku puzzle-based PV reconfiguration technique to lessen the impact of shading on panel efficiency. The work presented by the researchers in [19] demonstrated a power comparison method for PV array reconfiguration in shaded conditions to maximize power extraction. The researchers in [20] presented a reconfiguration method for the shaded PV array using the grasshopper optimization algorithm (GOA), aiming to enhance output power. To address the adverse effects of partial shading, the Marine Predators Algorithm (MPA) was employed to determine the optimal configuration of large-scale photovoltaic (PV) systems [21]. Yousri et al. [22] proposed a Multi-objective Grey Wolf Optimizer (MOGWO) for the optimal reconfiguration of shaded photo-voltaic arrays, enhancing power output by minimizing the row current difference, and outperformed earlier TCT and modified Sudoku methods. Mikkili et al. [23] underscored the advantage of Optimal Sudoku reconfiguration over traditional TCT and Sudoku for enhancing the power output and decreasing power loss under varying shading conditions, with results validated in MATLAB. The reserchers in [24] introduced Knight's tour, a unique reconfiguration method based on the movements of a chess knight, proven to be effective in maximizing power extraction from PV arrays under partial shading conditions, outperforming other traditional and puzzle-based methods across scenarios. To address the problems of existing optimization algorithms, in search of more straightforward and faster algorithms, research is being conducted to construct efficient algorithms for the application of PV reconfiguration.

Fang and Yang [25] designed a strategy for the dynamic reconfiguration of PV arrays with the objective of minimizing mismatch losses, particularly under partially shaded conditions. Their solution centers on mitigating the power losses caused by non-uniform irradiance through adaptive reconnection of PV module interlinks. By real-time adjustment of array configurations, the system surpasses traditional static setups in energy output and efficiency. The work in [26] presents the multidisciplinary Pelican Optimization Algorithm (POA), which optimally reforms heterogeneous rural rooftop PV arrays. The researchers' approach considers challenges due to changing rooftop orientations and module types with the goals of power output, shading impact, and reconfiguration cost optimization. The approach proposed improves PV system performance in autonomous complex rural environments through smart and self-adaptive array modification. In an alternative method, Sharma et al. [27] proposed a machine-learning model with the goal of increasing power retrieval via smart SPV array reconfiguration in industrial settings. Such an array optimization employs an AI-based mechanism derived from environmental factors like irradiance and temperature, which feeds into a supervised learning model that forecasts the best configuration. This algorithmic approach uses a model to provide instantaneous and context-sensitive reconfiguration choices that improve performance while reducing necessary calculations relative to classical methods. Hachemi et al. [28]

focused on overcoming the issues associated with modern distribution networks incorporating PV systems by suggesting a combined approach of dynamic network reconfiguration along with D-STATCOM deployment. Their focus was on improving the operational performance and voltage dynamics along with the power quality of distribution grids with high levels of PV penetration. Moreover, increasing distributed PV generation results in more challenges, such as excessive voltage, reverse flow power, and unbalanced load, which require advanced control methodologies.

However, many of the traditional reconfiguration techniques do not apply in urban PV systems where the modules have different orientations, tilts, and exposure to sunlight due to the addressable complexity. For that reason, the authors in [29] developed a multivariate optimization framework that takes into account power output, shading impact, cost of reconfiguration, and other relevant multi-performance metrics. This methodology is based on adaptive strategies to improve solution diversity and convergence of the modified metaheuristic as provided in the INGO algorithm. This algorithm assesses a large number of reconfiguration options and determines the best electrical connections among modules, which results in the maximization of energy output. The results of this simulation show that the method provided is of higher efficiency, adaptability, and computational performance when compared to conventional methods. It is shown how optimization inspired by nature can be effectively used for solving unsolved complex designed PV array problems, especially in the urban constrained environment. It is in line with the broader goal of improving intelligent management techniques with regard to PV array systems, where highly dynamic real-life conditions need to be considered. The researchers in [30] proposed a modified Chess Knight Reconfiguration (CKR) technique where the algorithm spaced shaded and unshaded modules within the array in a way that improves the uniformity of current flowing across layers. The algorithm determines performance metrics, total power output, and reduction in mismatch losses to analyze the pattern reconfigurations. The proposed approach outperformed traditional methods in reducing mismatch losses and improving system efficiency overall after extensive simulations on standard PV array configurations. In addition, the CKR method is straightforward to implement, and its computational efficiency makes it appropriate for real-time applications. This research demonstrates the promise that heuristic, grid-based approaches hold in intelligent PV array reconfiguration amid dynamic changes in environmental conditions. The researchers in [31] presented a PV reconfiguration method based on a hybrid method that combines the harmony search algorithm with a switching matrix framework using module interconnection evaluation and selection. This permits adaptive configuration of the PV system to changing patterns of irradiance. The algorithm also aims to obtain the configurations that yield maximum power output while seeking minimum computational time, cost of reconfiguration, and incurred computational expense. Simulation results confirmed that the proposed method outperformed traditional techniques, including TCT and Sudoku-based approaches, in power efficiency and reliability under diverse shading scenarios [32]. The researchers proposed an improved salp swarm algorithm (ISSA) that used tent chaotic initialization and a hybrid of Levy flight and lion swarm strategies to enhance MPPT accuracy and speed under PSCs. Simulations showed that ISSA outperforms conventional methods, achieving the highest accuracy and fastest tracking time.

In this article, the cuckoo search (CS) optimizer is utilized to provide the optimal design for the switching matrix to tackle the problem of modifying the weights of the objective function to guarantee the reliability and efficiency of the system. Using the proposed approach, we aim to minimize the contrast between the maximum and minimum row current levels. The introduced CS is applied to a series of shade patterns over a 9×9 PV array. The obtained results by CS are compared with SuDoKo,

modified SuDoKo, TCT, and MOGWO strategies through several statistical measures to appraise the performance of the proposed method. The results demonstrate the excellence of CS in creating the highest power values and smooth PV characteristics.

The remaining parts of the papers are organized as follows: In Section 2.1, we present the implemented PV equivalent circuit. In Section 2.2, we introduce evaluating performance for statistical metrics. The TCT scheme justification is documented in section 2.3. A brief description of CS is provided in section 2.4, while the proposed CS method with the executed objective functions is described in section 2.5. In Section 3, we present the results and the analysis of the CS-based reconfiguration system under the studied shade patterns. The conclusion is provided in Section 4.

2. Materials and methods

2.1. Modeling PV modules

The effectiveness of any PV plant is defined by the efficiency of the PV modules used in the system. A PV module is formed by merging many PV cells. The PV cell is the most basic element of PV systems. As a result, researchers prioritize the modeling of PV cells. Furthermore, modeling the non-linear behavior of PV cells becomes a difficult task [33]. A three types of diode models for improving power generation by undertaking multiple experiments: Single-diode (SD), double-diode (DD) were developed in [34,35], and three-diode model (TD) [36]. Because of its extensive capabilities, SD is the most commonly used of these three types [27]. We picked the single diode model for the creation of a PV array in this study because it is simple in design, has fewer parameters, and is the most extensively used model in real-time applications. The SD is comprised of five parameters: Ip_v, I_0, R_s, a, and R_p. The SD electrical model is created by combining all of these factors. Figure 1 illustrates the SD representation. Eq 1 provides the I − V properties of SD.

$$I = I_{pv} - I_0\left(exp\left(\frac{q(v + R_sI)}{akT}\right) - 1\right) - \frac{(v + R_sI)}{R_p} \tag{1}$$

where I_{pv} and v are the PV cell's measured I-V data, and I is the total amount of current produced by the PV cell. q is electron charge ($1.602 * 10^{-19}$ C), I_0 is the leakage current of a diode, Boltzmann constant k (1.38065031023J/K), and T is the Kelvin temperature. a is the ideality factor, R_s, and R_p are series and shunt resistances, respectively.

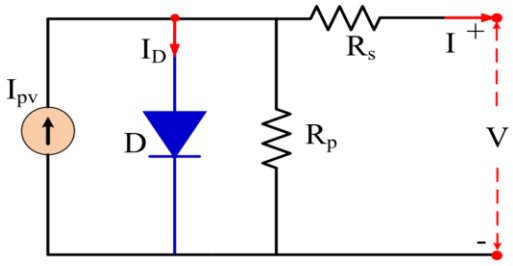

Figure 1. Electrical circuit of single diode PV model.

2.2. Metrics for evaluating performance

The most important part of any method's performance is its evaluation. Thus, the efficacy and

effectiveness of each approach, as well as the comparison of multiple ways, are acquired by evaluating the results of their performance. In this article, the performance of each approach is evaluated using various indicators after applying the introduced methods to various PV arrays to reconfigure and disperse the shadow. In this study, the global maximum power point (GMPP), fill factor (FF), mean loss (ML), and efficiency are introduced and used as performance evaluation indicators. Each of the aforementioned indicators is defined and calculated as follows:

- GMPP is calculated by computing the generated current in each row of the PV array.
- FF is one of the defining factors in the overall behavior of a solar cell and measures the area of a PV array module. The FF is determined by the maximum power point (p_m), open-circuit voltage (v_{OC}), and short circuit current (I_{s_C}). It can be calculated as follows [28–31]:

$$FF = \frac{p_m}{v_{OC} * I_{s_C}} \tag{2}$$

- The difference between the maximum power under uniform radiation (MPP_{uni}) and the GMPP under PSC ($GMPP_{Psc_s}$) is represented by ML. The ML can be calculated as follows:

$$ML = \frac{MPP_{uni} \ - \ GMPP_{Psc_s}}{GMPP_{Psc_s}} \tag{3}$$

- Efficiency (η) is defined as the ratio of the maximum power point (P_m) to the solar energy input (P_{in}). The efficiency can be stated mathematically as follows:

$$\eta = \frac{P_m}{P_{in}} \tag{4}$$

2.3. Metrics for evaluating performance

TCT is the most commonly utilized type of PV connection to achieve the rated amount of power. Following multiple assessments of various connection systems, the TCT is regarded as an excellent connection approach for PV projects. TCT connections are restricted to connecting cross-ties across each row of a series-parallel connection [31]. To validate the proposed CS technique, we used a 9 ×9 TCT PV array in this work. The TCT scheme is depicted in Figure 2. There are 9 rows and 9 columns in this TCT-connected scheme. Every PV module is represented by x and y, where x and y are row and column numbers, respectively. Equations 5 and 6 can be used to calculate the total current and the voltage of a TCT-connected PV array [31].

$$I_{out} = \sum_{y=1}^{9} I_{xy}, \ x=1,2...8,9 \tag{5}$$

$$v_{array} = \sum_{x=1}^{9} v_{m_x} \tag{6}$$

where I_{out} is the total current produced by the PV array, v_{array} is the total voltage that appears across the PV array terminals, and v_{m_x} is the PV module voltage at row x.

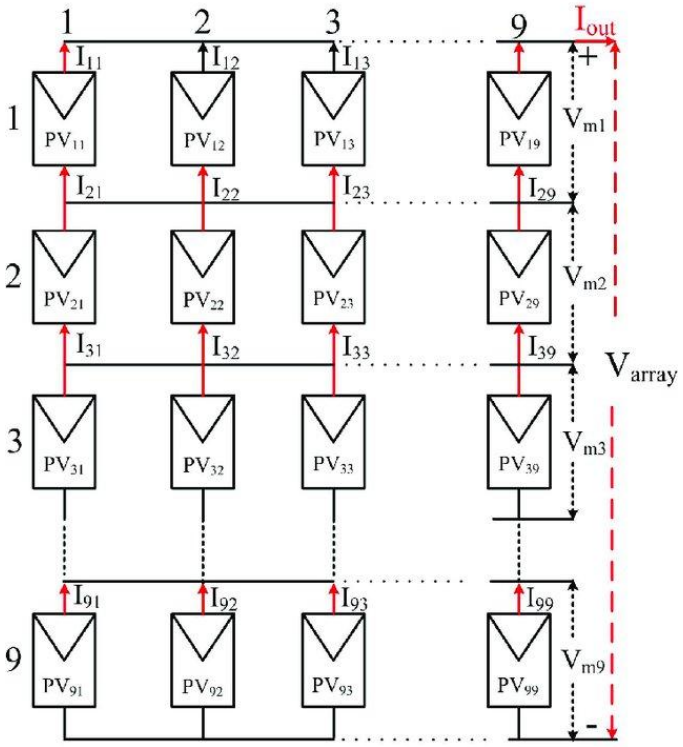

Figure 2. TCT connected 9 ×9 PV array structure.

The occurrence shadow should scatter routinely around the surface of the PV modules to achieve the most extreme power from the considered PV array. A typical TCT scheme cannot provide a uniform distribution of partial shading. We used CS to achieve uniform shade distribution and to increase power generation by discovering the ideal switching pattern. To carry out the suggested technique, a 9 ×9 TCT-linked system is created using a solar PV model with an open circuit voltage (v_{ocn}) of 49.5 (V) and a short circuit current (I_{sc}) of 8.6 (A). Temperature coefficients: K_v = -0.3624 × v_{ocn} and K_i = 0.071 × I_{sc}. The details of the proposed algorithms and the reconfiguration optimization process are described in the following section. To implement the suggested technique, a 9 ×9 TCT-linked system is built using a PV model with a voltage for open circuits (v_{ocn}) of 49.5 V and a current during a short circuit (I_{sc}) of 8.6 A. Temperature coefficients: K_v = -0.3624 × v_{ocn} and K_i = 0.071× I_{sc}. In the following section, we describe the algorithms suggested in depth, as well as the reconfiguration optimization process.

2.4. Cuckoo search algorithm

The CS method was first introduced by Yang and Deb in 2009 [37], which was inspired by the breeding habits of the cuckoo species. When CS is used, there are three basic standards. In each iteration, each cuckoo first lays a single egg before picking a nest at random to place it in. Second, the best nest and best solution would be transmitted to the successive layer. Third, a host bird finds the alien egg with a probability of P_ a∈ [0,1] utilizing the constant number of host nests [32]. The following L évy flight in (7) is:

$$x_i^{t+1} = x_i^t + \alpha \oplus \text{Levy}(\lambda) \tag{7}$$

where $X_i = [x_1, x_{2,} x_3, \ldots x_D]$, D is the problem dimension, α > 0 is the step size, ⊕ the product,

$\lambda > 0$ is the problem's scale, as represented by the step size, and the sequence number is represented by t. Multiplication by entries is represented by the symbol in the product, and Lévy (λ) generates a random walk with step lengths that are chosen at random from a Lévy range, as demonstrated in (8).

$$Lévy(\lambda) \approx t^{-\lambda}, (1 < \lambda \leq 3) \tag{8}$$

2.5. The proposed objective function

The PV reconfiguration optimization task aims to maximize the harvested power from the available PV array while reducing variation among row current values to provide smooth PV characteristics. In this setting, the work can be described as a goal optimization challenge with a conflict function that is objective. The suggested goal indicates one of the absolute differences between the highest and lowest row current values, as demonstrated in (9):

$$Min(Obj) = |I_{Max} - I_{Min}| \tag{9}$$

The objective of implementing the CS is to find the best structure design for the switch array that balances the aforementioned objective function. The goal function was designed to maximize the generated power; the form was created to ensure uniform distribution of shade on the surface of the considered array. The best non-dominated solutions so far obtained by the objective optimization methods are archived. The best answer can be chosen using some techniques. Among the acquired solution vectors in this investigation, a switch matrix pattern with the smallest difference in the current levels of the rows is judged to be the best solution, enabling the designer to choose the best outcome. To ensure that the best solution is obtained, the process is repeated 500 times. The CS kicks in anytime the system's output power falls below 80% of gathered power at standard irradiation and temperature conditions (1000 W/m^2 and 25℃). The proposed steps for reconfiguring the partially shaded PV array can be explained as follows:

Step 1: Initialize radiation pattern matrix G (9*9) and initialize nests with random matrix arrangements.
Step 2: Evaluate the objective function for each nest.
Step 3: Repeat for a specified number of iterations.

- For each nest:
  - Generate a new cuckoo (solution) by randomizing the matrix vertically.
  - Calculate the objective function for the new cuckoo.
  - Choose a random nest and compare the new cuckoo with it.
  - If the new cuckoo has a better score, replace the nest with the new cuckoo.
- Abandon the worst nests and generate new ones:

Step 4: Find the best solution with the minimum difference between row currents using Eqs (10-16).
Step 5: Store the optimal arrangement and position changes.
Step 6: Calculate output voltage and output power based on the optimal arrangement and row currents.
Step 7: Return the optimal arrangement, minimum difference, position changes, output voltage, and output power.

3. Results and discussion

The performance of the CS is evaluated in this section over a variety of partial shade patterns across a 9 × 9 PV array. The provided shadow covers 4 × 4 the investigated array's space, and incident irradiance values range from 100 W/m^2 to 1000 W/m^2. The proposed approach is compared to TCT, Sudoku, Optimal Sudoku, and MOGWO arrangements to illustrate its superiority in delivering the highest power value and the minimum current difference between each row with a regular distribution for the shade over the array surface. For the comparison stage, many statistical metrics are used: 1) Mismatch power loss ML (%), 2) Fill factor FF (%), and 3) efficiency η (%). The test is run on a laptop with 16 GB of RAM and a Core i7 processor running at 2.30 GHz, and the MATLAB 2022 edition.

Case 1: Bottom right corner 4 × 4 sub-arrays

In this case, the bottom right quadrant of panel 4 × 4 is shaded with 600 W/m^2 and 400 W/m^2, whereas the remaining PV modules receive full irradiation, or 1000 W/m^2, as shown in Figure 2(a). Various TCT schemes, including achieved Sudoku, Sudoku with dispersed shade, Optimal Sudoku, dispersed shade Optimal Sudoku, MOGWO, and the suggested CS, are shown in Figure 3(b to g). The currents generated by all rows of the TCT system are calculated. Sudoku, Optimal Sudoku, MOGWO, and CS are necessary to determine the global maximum power. As shown in Figure 3(a), the PV panels in rows 1 through 5 get the same quantity of radiation, or 1000 W/m^2. As a result, the current generated by these five rows are be equal. The row currents may theoretically be determined as in (10).

$$I_{Rw_1}\ to\ I_{Rw_5}=A_{11}I_{11}+A_{12}I_{12}+A_{13}I_{13}+ - - -A_{19}I_{19.} \tag{10}$$

Here, $A_{11}=\frac{G_{11}}{G_0}=1$, $G_{11}$and I_{11} represent the input irradiance and the current produced by the PV module 11. G_0 represents the standard irradiation, which is 1000 W/m^2. Each module's current at complete irradiation might be designated as IM. As a result, the current from row 1 to row 5 can be calculated as shown in (11).

$$I_{Rw_1}\ to\ I_{Rw_5}=9\left(\frac{1000}{1000}\right)I_M=9I_M \tag{11}$$

Similarly, the currents of the rows that remain can be estimated in the following way:

Row current for $I_{R\omega_6}$and $I_{R\omega_7}$. Rows can be given as in (12):

$$I_{Rw_6}=I_{Rw_7}=5\left(\frac{1000}{1000}\right)I_M+2\left(\frac{600}{1000}\right)I_M+2\left(\frac{400}{1000}\right)I_M=7I_M \tag{12}$$

Row current for $I_{R\omega_8}$ and $I_{R\omega_9}$. The rows are as in (13):

$$I_{Rw_8}=I_{Rw_9}=5\left(\frac{1000}{1000}\right)I_M+4\left(\frac{600}{1000}\right)I_M=7.4I_M \tag{13}$$

Following the same processes as in Figure 3(a), the dispersed shadow pattern of the proposed CS scheme can be given as in (14):

$$I_{Rw_1}=I_{Rw_2}=I_{Rw_4}=I_{Rw_5}=I_{Rw_7}=7\left(\frac{1000}{1000}\right)I_M+2\left(\frac{600}{1000}\right)I_M=8.2I_M \tag{14}$$

The row current for I_{Rw_3} and I_{Rw_6}. Rows can be calculated as in (15):

$$I_{Rw_3} = I_{Rw_6} = 7\left(\frac{1000}{1000}\right)I_M + \left(\frac{600}{1000}\right)I_M + \left(\frac{400}{1000}\right)I_M = 8I_M \quad (15)$$

The row current for I_{Rw_8} and I_{Rw_9}. Rows can be calculated as in (16):

$$I_{Rw_8} = I_{Rw_9} = 8\left(\frac{1000}{1000}\right)I_M + \left(\frac{400}{1000}\right)I_M = 8.4I_M \quad (16)$$

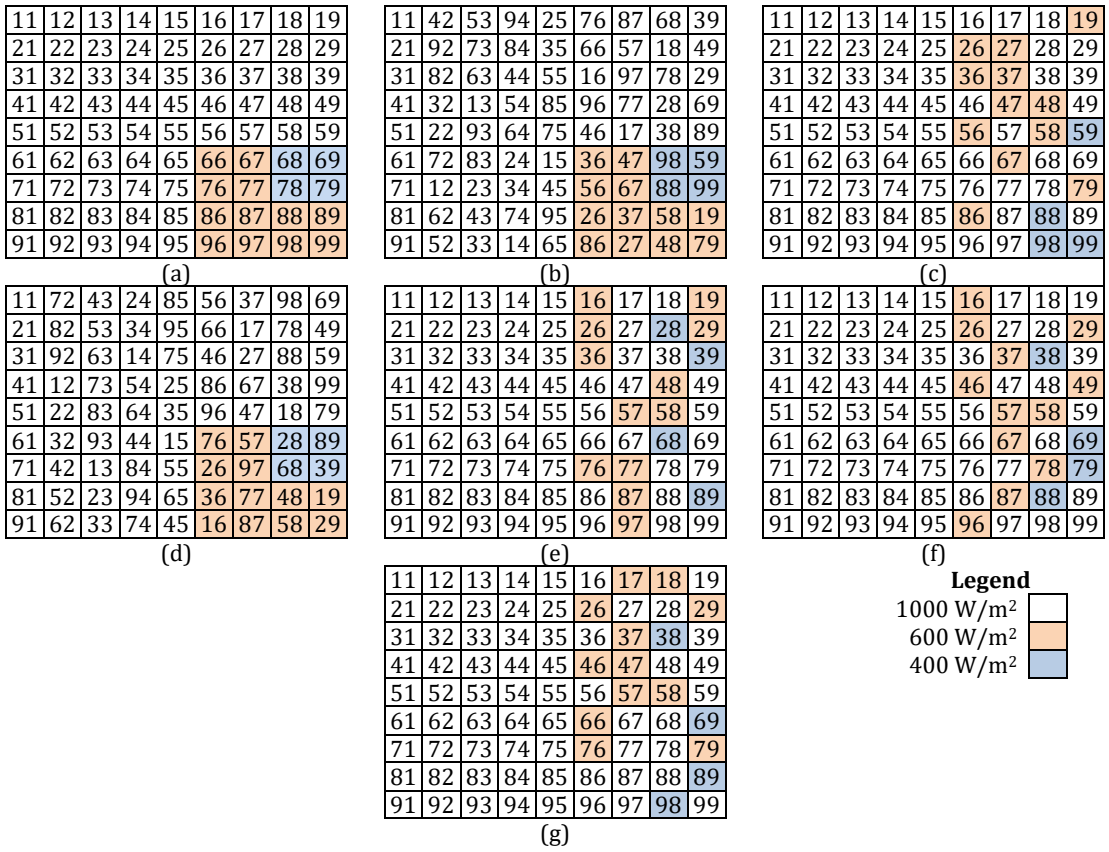

Figure 3. Results of case 1. (a) TCT scheme, (b) Sudoku arrangement, (c) Shade dispersion in Sudoku arrangement, (d) Optimal Sudoku arrangement, (e) Shade dispersion in Optimal Sudoku arrangement, (f) MOGWO, and (g) the proposed CS.

Table 1 demonstrates the acquired voltage and power tracked using TCT, Sudoku, Optimal Sudoku, MOGWO, and the suggested CS after the current calculations. The comparison provided by the CS and MOGWO methods generates the highest increased power of $72v_m I_m$. Furthermore, the recommended CS and MOGWO have only three powers, whereas Sudoku has five power values. This indicates the presence of several peaks in the P-V curve. When multiples exist in the PV curves, it generates less electricity. Sudoku and Optimal Sudoku generate $68.4v_m I_m$ of power, and this is somewhat higher for TCT but results in more multiple peaks of TCT-connected systems. Figure 4 indicates the multiple peaks and power. According to the results, the proposed CS obtained 23.6071 kW from the reconfigured PV array, in contrast to the MOGWO, Optimal Sudoku, Sudoku, and TCT yielding 23.5365 kW, 23.2966 kW, 23.2567 kW, and 21.8567 kW, respectively. The acquired parameters, such as ML (%), FF (%), and (%), are graphically shown in Figure 5.

Table 1. Analysis of TCT, Sudoku, Optimal Sudoku, MOGWO, and CS schemes of case 1.

TCT				Sudoku				Optimal Sudoku			
I_{R_i}	$I(A)$	$V(V)$	$P(W)$	I_{R_i}	$I(A)$	$V(V)$	$P(W)$	I_{R_i}	$I(A)$	$V(V)$	$P(W)$
I_{R_7}	$7I_m$	$9v_m$	$63v_m I_m$	I_{R_5}	$7.6I_m$	$9v_m$	$68.4v_m I_m$	I_{R_2}	$7.6I_m$	$9v_m$	$68.4v_m I_m$
I_{R_6}	-	-	-	I_{R_9}	$7.8I_m$	$8v_m$	$62.4v_m I_m$	I_{R_8}	$8I_m$	$8v_m$	$64v_m I_m$
I_{R_9}	$7.4I_m$	$7v_m$	$51.8v_m I_m$	I_{R_8}	$8I_m$	$7v_m$	$56v_m I_m$	I_{R_3}	-	-	-
I_{R_8}	-	-	-	I_{R_4}	$8.2I_m$	$6v_m$	$49.2v_m I_m$	I_{R_7}	$8.2I_m$	$6v_m$	$49.2v_m I_m$
I_{R_5}	$9I_m$	$5v_m$	$45v_m I_m$	I_{R_3}	-	-	-	I_{R_5}	-	-	-
I_{R_4}	-	-	-	I_{R_2}	-	-	-	I_{R_1}	-	-	-
I_{R_3}	-	-	-	I_{R_7}	$8.6I_m$	$3v_m$	$25.8v_m I_m$	I_{R_6}	$8.4I_m$	$3v_m$	$25.2v_m I_m$
I_{R_2}	-	-	-	I_{R_6}	-	-	-	I_{R_9}	$8.6I_m$	$2v_m$	$17.2v_m I_m$
I_{R_1}	-	-	-	I_{R_1}	-	-	-	I_{R_4}	-	-	-

MOGWO				Proposed CS			
I_{R_i}	$I(A)$	$V(V)$	$P(W)$	I_{R_i}	$I(A)$	$V(V)$	$P(W)$
I_{R_8}	$8I_m$	$9v_m$	$72v_m I_m$	I_{R_6}	$8I_m$	$9v_m$	$72v_m I_m$
I_{R_7}	-	-	-	I_{R_3}	-	-	-
I_{R_6}	-	-	-	I_{R_7}	$8.2I_m$	$7v_m$	$57.4v_m I_m$
I_{R_3}	-	-	-	I_{R_5}	-	-	-
I_{R_5}	$8.2I_m$	$5v_m$	$41v_m I_m$	I_{R_4}	-	-	-
I_{R_4}	-	-	-	I_{R_2}	-	-	-
I_{R_2}	-	-	-	I_{R_1}	-	-	-
I_{R_9}	$8.6I_m$	$2v_m$	$17.2v_m I_m$	I_{R_9}	$8.4I_m$	$2v_m$	$16.8v_m I_m$
I_{R_1}	-	-	-	I_{R_8}	-	-	-

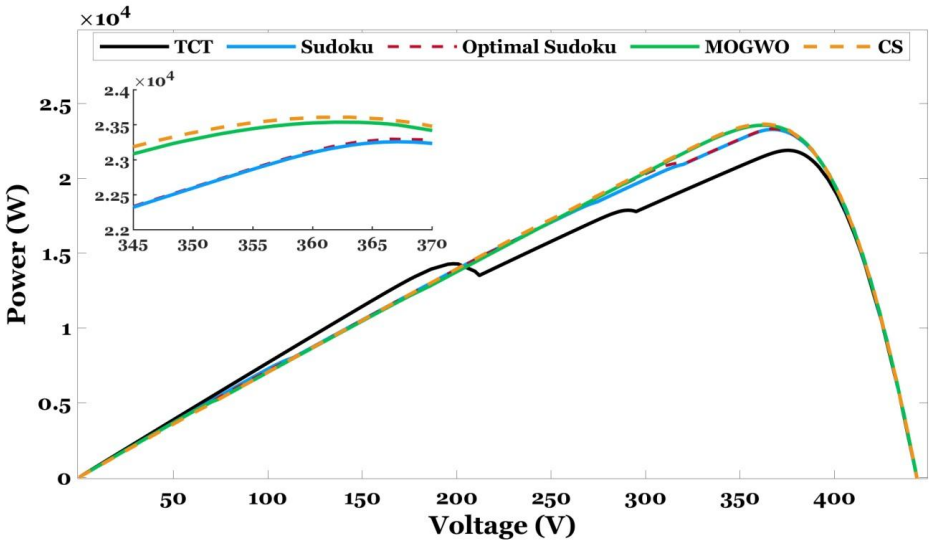

Figure 4. Characteristics of case 1 in terms of P-V.

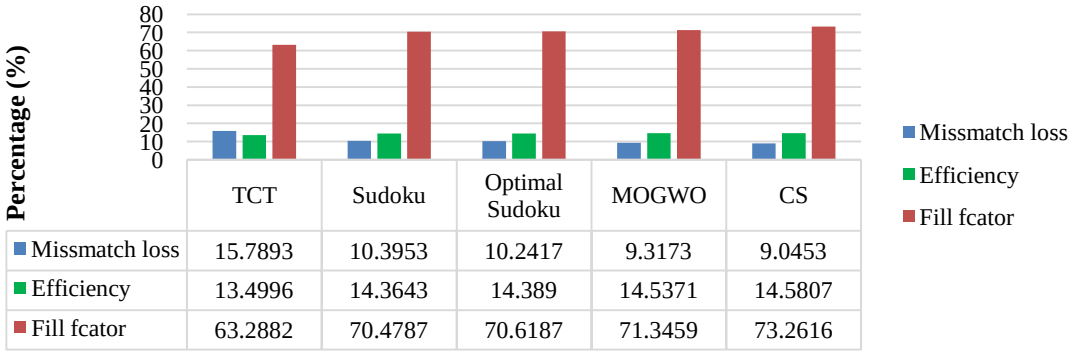

	TCT	Sudoku	Optimal Sudoku	MOGWO	CS
Missmatch loss	15.7893	10.3953	10.2417	9.3173	9.0453
Efficiency	13.4996	14.3643	14.389	14.5371	14.5807
Fill fcator	63.2882	70.4787	70.6187	71.3459	73.2616

Figure 5. FF, ML, and efficiency for case 1.

Case 2: Bottom left corner 4 × 4 sub-arrays

The bottom left c quadrant of a 4 × 4 panel of PV cells is shaded by four degrees of irradiation: 1000 W/m^2, 700 W/m^2, 400 W/m^2, and 300 W/m^2, as shown in Figure 6. Its redesigned shadow patterns created fromTCT, Sudoku, Optimal Sudoku, MOGWO, and CS are shown in Figure 5(b to g).

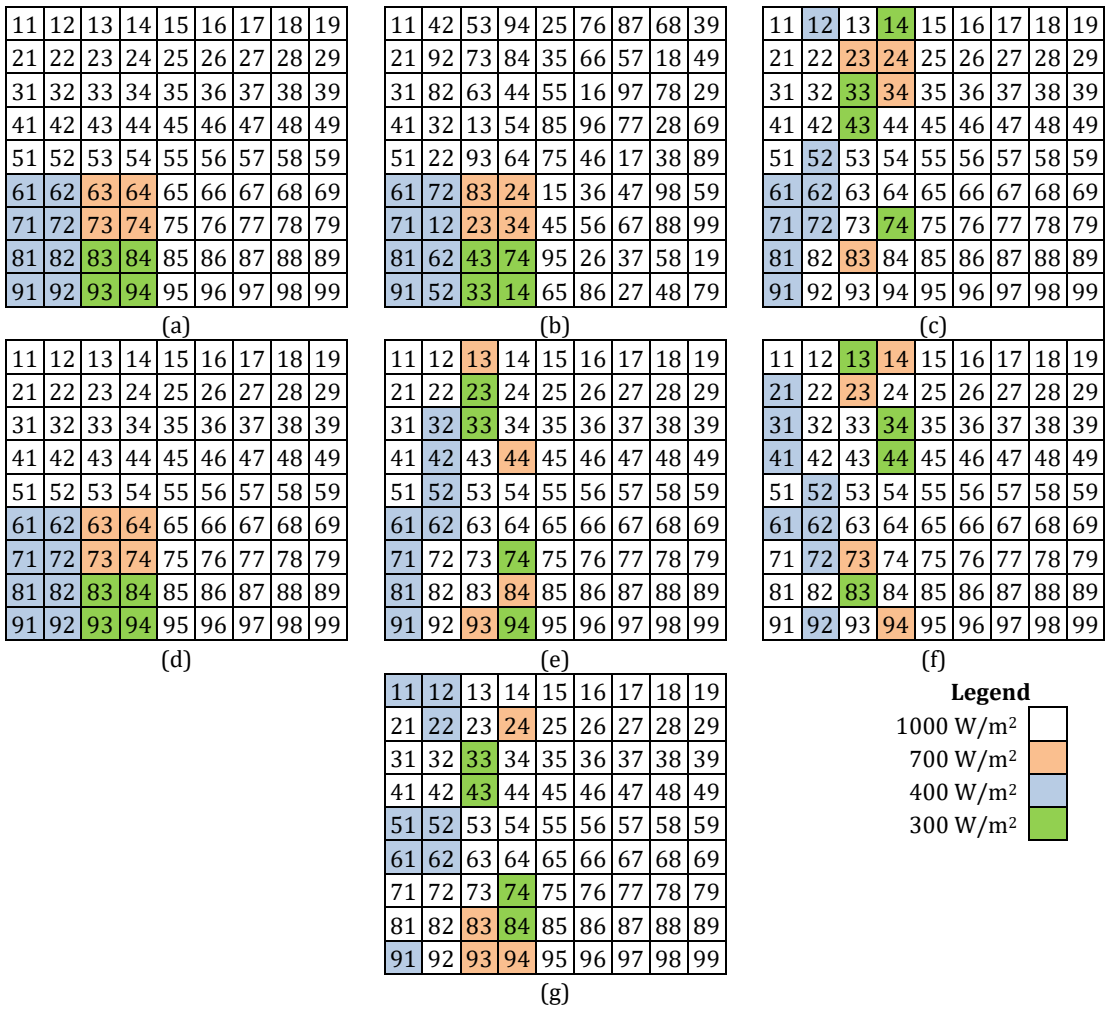

Figure 6. Results of case 2. (a) TCT scheme, (b) Sudoku arrangement, (c) Shade dispersion in Sudoku arrangement, (d) Optimal Sudoku arrangement, (e) Shade dispersion in Optimal Sudoku arrangement, (f) MOGWO, and (g) the used CS.

Table 2 shows the voltage and power created by computing the currents generated by any row of the five techniques investigated. Moreover, the suggested CS approach yields a large amount of power compared to the other methods considered in this study. Furthermore, it produces fewer power variations, which improves the delivered power from PV. Figure 7 displays the P-V curves for TCT situation 2 with dispersed shade patterns. The GMPP obtained using the method suggested by CS, MOGWO, Optimal Sudoku, Sudoku, and TCT are determined to be 23.0057 kW, 22.9688 kW, 22.6788 kW, 22.2464 kW, and 20.3282 kW, respectively. The MOGWO is ranked second in flow, with a generated power of 22.9688 kW. The shade dispersed utilizing a CS-based arrangement confronts the multi-peaks and achieves a distinct peak, a critical discovery made from the P-V curve. More importantly, the obtained GMPP is nearly identical to the nominal operating voltage**.** The TCT features show that a change in irradiation levels induces bypassing of PV modules, resulting in a current differential that forms several peaks in the PV curves, as shown in Figure 7. Furthermore, its global power is vastly different from the GMPP. The obtained parameters, such as M (%), FF (%), and η (%), for all PV array configurations are depicted in Figure 8.

Table 2. Analysis of TCT, Sudoku, Optimal Sudoku, MOGWO, and CS schemes of case 2.

TCT				**Sudoku**				**Optimal Sudoku**			
I_{R_i}	$I(A)$	$V(V)$	$P(W)$	I_{R_i}	$I(A)$	$V(V)$	$P(W)$	I_{R_i}	$I(A)$	$V(V)$	$P(W)$
I_{R_9}	$6.4I_m$	$9v_m$	$57.6v_m I_m$	I_{R_7}	$7.1I_m$	$9v_m$	$63.9v_m I_m$	I_{R_9}	$7.4I_m$	$9v_m$	$66.6v_m I_m$
I_{R_8}	-	-	-	I_{R_1}	$7.7I_m$	$8v_m$	$61.6v_m I_m$	I_{R_7}	$7.7I_m$	$8v_m$	$61.6v_m I_m$
I_{R_7}	$7.2I_m$	$7v_m$	$50.4v_m I_m$	I_{R_6}	$7.8I_m$	$7v_m$	$54.6v_m I_m$	I_{R_3}	-	-	-
I_{R_6}	-	-	-	I_{R_3}	$8I_m$	$6v_m$	$48v_m I_m$	I_{R_6}	$7.8I_m$	$6v_m$	$46.8v_m I_m$
I_{R_5}	$9I_m$	$5v_m$	$45v_m I_m$	I_{R_8}	$8.1I_m$	$5v_m$	$40.5v_m I_m$	I_{R_8}	$8.1I_m$	$5v_m$	$40.5v_m I_m$
I_{R_4}	-	-	-	I_{R_4}	$8.3I_m$	$4v_m$	$33.2v_m I_m$	I_{R_4}	-	-	-
I_{R_3}	-	-	-	I_{R_9}	$8.4I_m$	$3v_m$	$25.2v_m I_m$	I_{R_2}	$8.3I_m$	$3v_m$	$24.9v_m I_m$
I_{R_2}	-	-	-	I_{R_5}	-	-	-	I_{R_5}	$8.4I_m$	$2v_m$	$16.8v_m I_m$
I_{R_1}	-	-	-	I_{R_2}	-	-	-	I_{R_1}	$8.7I_m$	$1v_m$	$8.7v_m I_m$

MOGWO				**Proposed CS**			
I_{R_i}	$I(A)$	$V(V)$	$P(W)$	I_{R_i}	$I(A)$	$V(V)$	$P(W)$
I_{R_4}	$7.7I_m$	$9v_m$	$69.3v_m I_m$	I_{R_9}	$7.8I_m$	$9v_m$	$70.2v_m I_m$
I_{R_3}	-	-	-	I_{R_6}	-	-	-
I_{R_6}	$7.8I_m$	$7v_m$	$54.6v_m I_m$	I_{R_5}	-	-	-
I_{R_1}	$8I_m$	$6v_m$	$48v_m I_m$	I_{R_1}	-	-	-
I_{R_9}	$8.1I_m$	$5v_m$	$40.5v_m I_m$	I_{R_8}	$8.1I_m$	$5v_m$	$40.5v_m I_m$
I_{R_7}	-	-	-	I_{R_2}	-	-	-
I_{R_2}	-	-	-	I_{R_7}	$8.3I_m$	$3v_m$	$24.9v_m I_m$
I_{R_8}	$8.3I_m$	$2v_m$	$16.6v_m I_m$	I_{R_4}	-	-	-
I_{R_5}	$8.4I_m$	$1v_m$	$8.4v_m I_m$	I_{R_3}	-	-	-

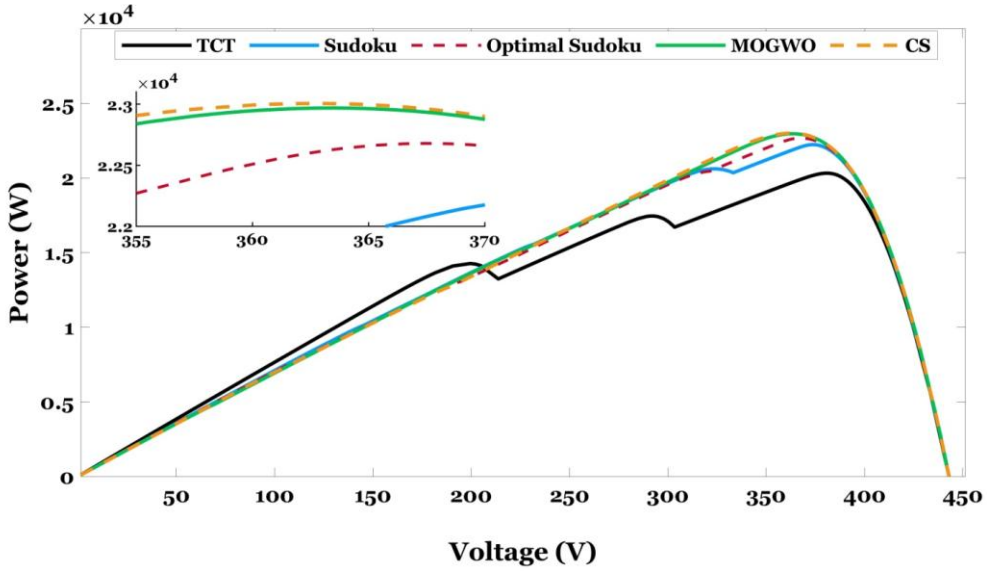

Figure 7. Characteristics of case 2 in terms of P-V.

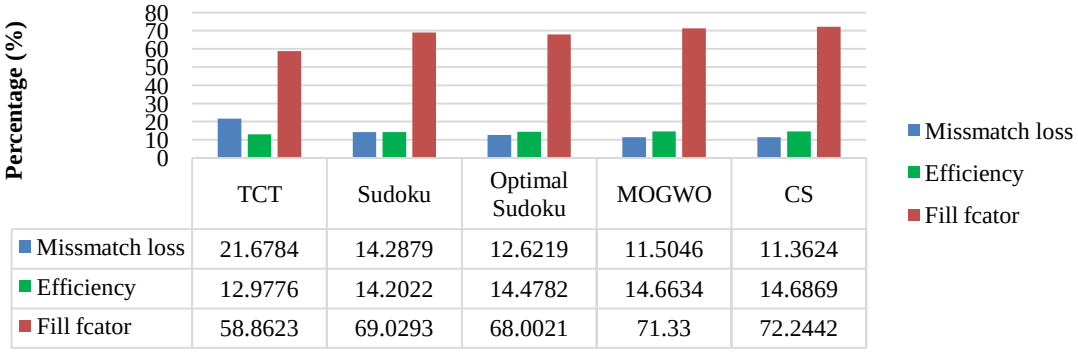

	TCT	Sudoku	Optimal Sudoku	MOGWO	CS
Missmatch loss	21.6784	14.2879	12.6219	11.5046	11.3624
Efficiency	12.9776	14.2022	14.4782	14.6634	14.6869
Fill fcator	58.8623	69.0293	68.0021	71.33	72.2442

Figure 8. FF, ML, and efficiency for case 2.

Case 3: Top left corner 4 × 4 sub-arrays

In this case, five irradiations are investigated to show the effectiveness of the suggested approach. As shown in Figure 9(a), the left top corner of the 4 × 4 PV array is shaded with irradiation levels of 500 W/m^2, 300 W/m^2, 200 W/m^2, and 100 W/m^2, while the remaining modules receive full irradiation of 1000W/m^2. Figure 9(b) to (g) display the Sudoku distributed shadow patterns, Optimal Sudoku, MOGW, and suggested CS, respectively. Theoretically, estimated current, voltage, and power levels are presented in Table 3, identical to the other instances. According to Table 3, the suggested CS creates 67.5 VmIm, while MOGWO, Optimal Sudoku, Sudoku, and TCT generate 66.6 VmIm, 59.4 VmIm, 65.7 VmIm, and 54 VmIm, respectively. Figure 10 depicts P-V curves simulated for this situation. The depicted curves show that the reconfigured CS method has demonstrated that even with a small, wide shadow pattern, it has maximum power. In this situation, the suggested CS generates 22.1083 kW of power, which is greater than MOGWO, optimal sudoku, sudoku, and TCT, which generate 22.0419 kW, 20.9088 kW, 21.9276 kW, and 18.9180 kW, respectively. The obtained parameters, such as ML (%), FF (%), and (%) for all PV array topologies are graphically shown in Figure 11.

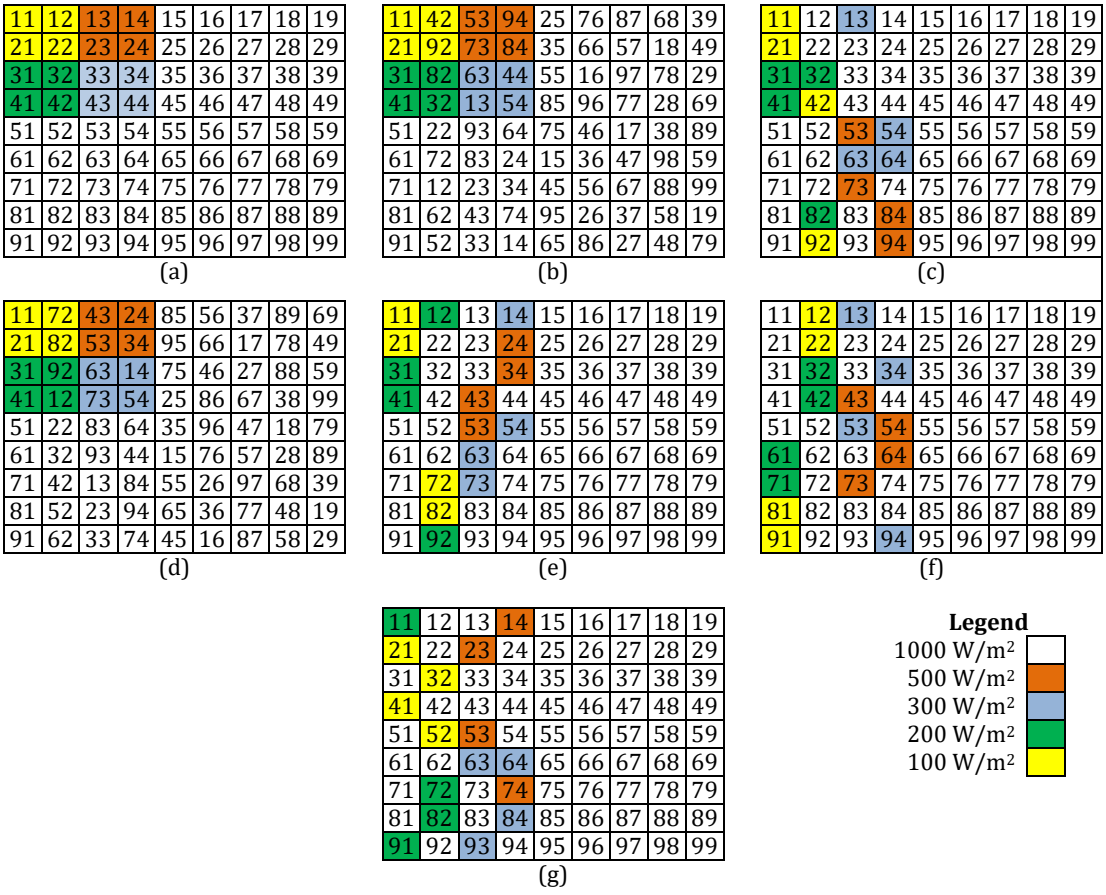

Figure 9. Results of case 3. (a) TCT scheme, (b) Sudoku arrangement, (c) Shade dispersion in Sudoku arrangement, (d) Optimal Sudoku arrangement, (e) Shade dispersion in Optimal Sudoku arrangement, (f) MOGWO, and (g) CS.

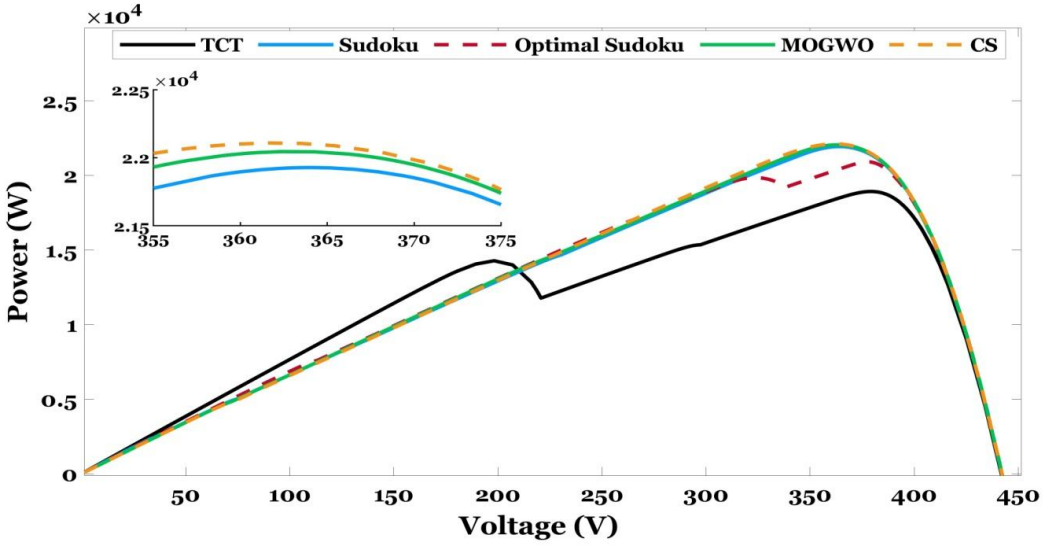

Figure 10. Characteristics of case 3 in terms of P-V.

Table 3. Analysis of TCT, Sudoku, Optimal Sudoku, MOGWO, and CS schemes of case 3.

TCT				Sudoku				Optimal suduko			
I_{R_i}	$I(A)$	$V(V)$	$P(W)$	I_{R_i}	$I(A)$	$V(V)$	$P(W)$	I_{R_i}	$I(A)$	$V(V)$	$P(W)$
I_{R_4}	$6I_m$	$9v_m$	$54v_m I_m$	I_{R_4}	$7.3I_m$	$9v_m$	$65.7v_m I_m$	I_{R_1}	$6.6I_m$	$9v_m$	$59.4v_m I_m$
I_{R_3}	-	-	-	I_{R_3}	$7.4I_m$	$8v_m$	$59.2v_m I_m$	I_{R_7}	$7.4I_m$	$8v_m$	$59.2v_m I_m$
I_{R_2}	$6.2I_m$	$7v_m$	$43.4 v_m I_m$	I_{R_1}	-	-	-	I_{R_2}	$7.6I_m$	7	$53.2v_m I_m$
I_{R_1}	-	-	-	I_{R_9}	$7.6I_m$	$6v_m$	$45.6v_m I_m$	I_{R_4}	$7.7I_m$	$6v_m$	$46.2v_m I_m$
I_{R_9}	$9I_m$	$5v_m$	$45v_m I_m$	I_{R_6}	-	-	-	I_{R_3}	-	-	-
I_{R_8}	-	-	-	I_{R_8}	$7.7I_m$	$4v_m$	$30.8v_m I_m$	I_{R_5}	$7.8I_m$	$4v_m$	$31.2v_m I_m$
I_{R_7}	-	-	-	I_{R_5}	$7.8I_m$	$3v_m$	$23.4v_m I_m$	I_{R_8}	$8.1I_m$	$3v_m$	$24.3v_m I_m$
I_{R_6}	-	-	-	I_{R_2}	$8.1I_m$	$2v_m$	$16.2v_m I_m$	I_{R_9}	$8.2I_m$	$2v_m$	$16.4v_m I_m$
I_{R_5}	-	-	-	I_{R_7}	$8.5I_m$	$1v_m$	$8.5v_m I_m$	I_{R_6}	$8.3I_m$	$1v_m$	$8.3v_m I_m$

MOGWO				CS			
I_{R_i}	$I(A)$	$V(V)$	$P(W)$	I_{R_i}	$I(A)$	$V(V)$	$P(W)$
I_{R_9}	$7.4I_m$	$9v_m$	$66.6v_m I_m$	I_{R_9}	$7.5I_m$	$9v_m$	$67.5v_m I_m$
I_{R_1}	-	-	-	I_{R_8}	-	-	-
I_{R_3}	$7.5I_m$	$7v_m$	$52.5v_m I_m$	I_{R_6}	$7.6I_m$	$7v_m$	$53.2v_m I_m$
I_{R_7}	$7.7I_m$	$6v_m$	$46.2v_m I_m$	I_{R_5}	-	-	-
I_{R_6}	-	-	-	I_{R_2}	-	-	-
I_{R_4}	-	-	-	I_{R_7}	$7.7I_m$	$4v_m$	$30.8v_m I_m$
I_{R_5}	$7.8I_m$	$3v_m$	$23.4v_m I_m$	I_{R_1}	-	-	-
I_{R_8}	$8.1I_m$	$2v_m$	$16.2v_m I_m$	I_{R_4}	$8.1I_m$	$2v_m$	$16.2v_m I_m$
I_{R_2}	-	-	-	I_{R_3}	-	-	-

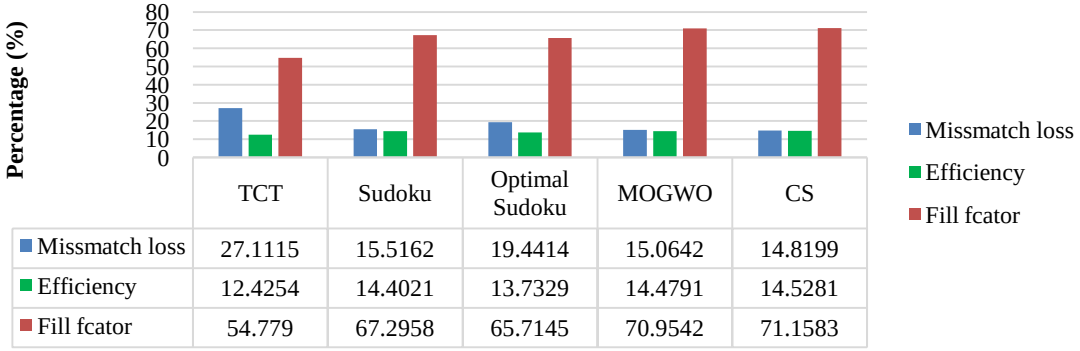

	TCT	Sudoku	Optimal Sudoku	MOGWO	CS
Missmatch loss	27.1115	15.5162	19.4414	15.0642	14.8199
Efficiency	12.4254	14.4021	13.7329	14.4791	14.5281
Fill fcator	54.779	67.2958	65.7145	70.9542	71.1583

Figure 11. FF, ML, and efficiency for case 3.

Case 4: Center 4 ×4 sub-array

In this case, the central section of the array is shaded at four different shade levels: 600 W/m^2, 400 W/m^2, 300W/m^2, and 400 W/m^2, while the remainder of the PV modules are uncovered and receive full irradiance 1000 W/m^2. Figure 12(a) depicts the arrangement of this shade pattern using the TCT-linked scheme. The dispersed shading condition is shown in Figures 12(b) to (g) after

reconfiguration using Sudoku, Optimal Sudoku, MOGWO, and the suggested CS technique. Table 5 shows the theoretical calculations for the respective currents, voltages, and powers. Figure 13 displays simulated P-V curves for this case. In this situation, due to the high and extensive shade circumstances, enormous peaks in the P-V curves of the TCT-connected system exist, and the system skips the shaded PV modules. As a result, the current difference is generated, which reflects on several peaks. Moreover, suggested CS eliminates PV module bypassing and achieves a unique global power of 22.6669 kW, which is significantly greater than MOGWO, Optimal sudoku, sudoku, and TCT, which generate 22.6077 kW, 22.0429 kW, 21.9933 kW, and 19.6928 kW, respectively. The obtained parameters, such as ML (%), FF (%), and η (%) for all PV array topologies, are graphically depicted in Figure 14.

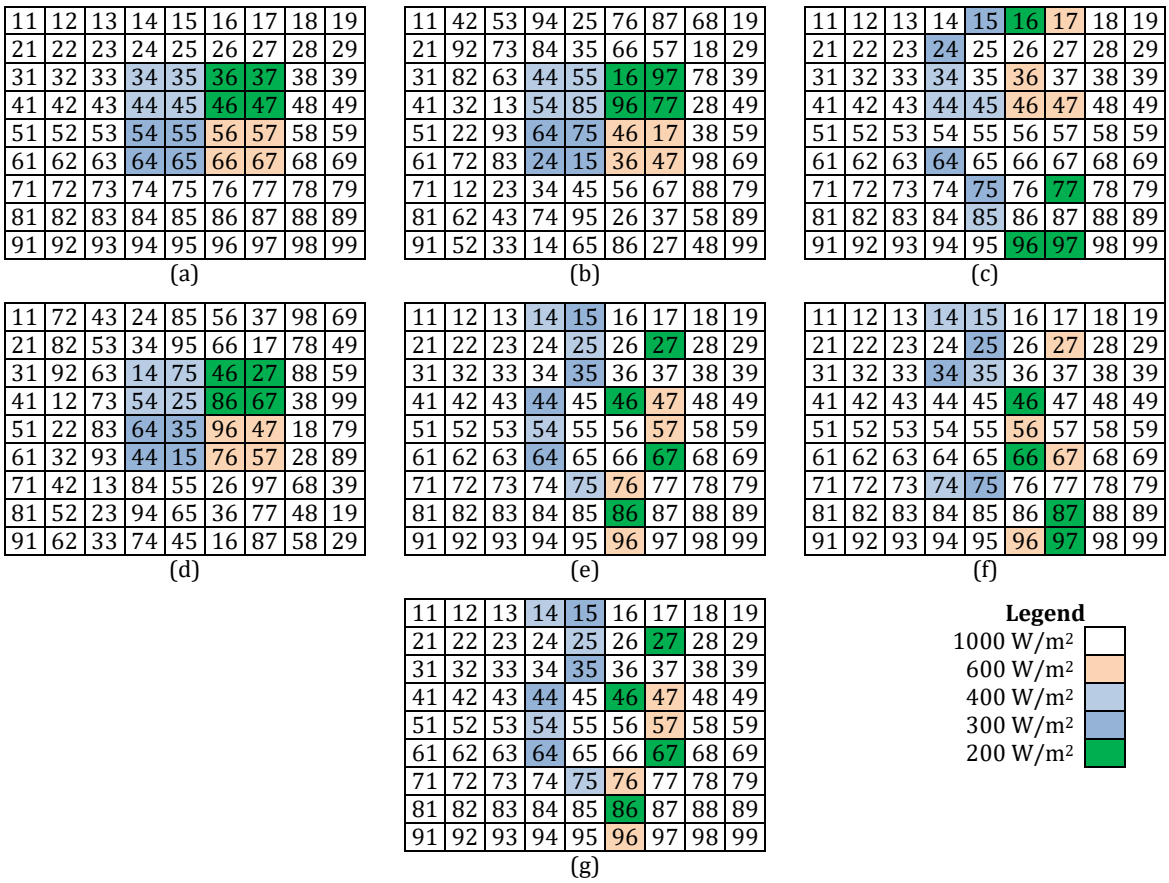

Figure 12. Results of case 4. (a) TCT scheme, (b) Sudoku arrangement, (c) Shade dispersion in Sudoku arrangement, (d) Optimal Sudoku arrangement, (e) Shade dispersion in Optimal Sudoku arrangement, (f) MOGWO, and (g) CS.

Case 5: Two 3 × 3 sub-arrays

To investigate system performance in various settings, an extensive variety of shade occurrences with two irradiance levels are considered. The two irradiation levels are 600 W/m^2 and 200 W/m^2, respectively, and their indication with a TCT approach may be seen in Figure 15(a). Because a new shade type is used in this circumstance, a clever reconfiguration strategy that contributes to a high shadow dispersion process must be recognized.

Table 4. Analysis of TCT, Sudoku, Optimal Sudoku, MOGWO, and CS schemes of case 4.

TCT				Sudoku				Optimal suduko			
I_{R_i}	$I(A)$	$V(V)$	$P(W)$	I_{R_i}	$I(A)$	$V(V)$	$P(W)$	I_{R_i}	$I(A)$	$V(V)$	$P(W)$
I_{R_3}	$6.2I_m$	$9v_m$	$55.8v_m I_m$	I_{R_1}	$7.1I_m$	$9v_m$	$63.9v_m I_m$	I_{R_4}	$7.1I_m$	$9v_m$	$63.9v_m I_m$
I_{R_4}	-	-	-	I_{R_9}	$7.4I_m$	$8v_m$	$59.2v_m I_m$	I_{R_6}	$7.5I_m$	$8v_m$	$60v_m I_m$
I_{R_6}	$6.8I_m$	$7v_m$	$47.6v_m I_m$	I_{R_7}	$7.5I_m$	$7v_m$	$52.5v_m I_m$	I_{R_2}	$7.6I_m$	$7v_m$	$53.2v_m I_m$
I_{R_5}	-	-	-	I_{R_4}	$7.6I_m$	$6v_m$	$45.6v_m I_m$	I_{R_1}	$7.7I_m$	$6v_m$	$46.2v_m I_m$
I_{R_9}	$9I_m$	$5v_m$	$45v_m I_m$	I_{R_5}	$7.8I_m$	$5v_m$	$39v_m I_m$	I_{R_7}	$8I_m$	$5v_m$	$40v_m I_m$
I_{R_8}	-	-	-	I_{R_6}	$8.3I_m$	$4v_m$	$33.2v_m I_m$	I_{R_5}	-	-	-
I_{R_7}	-	-	-	I_{R_2}	-	-	-	I_{R_8}	$8.2I_m$	$3v_m$	$24.6v_m I_m$
I_{R_2}	-	-	-	I_{R_8}	$8.4I_m$	$2v_m$	$16.8v_m I_m$	I_{R_3}	$8.3I_m$	$2v_m$	$16.6v_m I_m$
I_{R_1}	-	-	-	I_{R_3}	$8.6I_m$	$1v_m$	$8.6v_m I_m$	I_{R_9}	$8.6I_m$	$1v_m$	$8.6v_m I_m$

MOGWO				CS			
I_{R_i}	$I(A)$	$V(V)$	$P(W)$	I_{R_i}	$I(A)$	$V(V)$	$P(W)$
I_{R_8}	$7.6I_m$	$9v_m$	$68.4v_m I_m$	I_{R_7}	$7.7I_m$	$9v_m$	$69.3v_m I_m$
I_{R_5}	-	-	-	I_{R_3}	-	-	-
I_{R_7}	$7.7I_m$	$7v_m$	$53.9v_m I_m$	I_{R_9}	$7.8I_m$	$7v_m$	$54.6v_m I_m$
I_{R_4}	$7.9I_m$	$6v_m$	$47.4v_m I_m$	I_{R_6}	-	-	-
I_{R_2}	-	-	-	I_{R_1}	-	-	-
I_{R_1}	-	-	-	I_{R_5}	$7.9I_m$	$4v_m$	$31.6v_m I_m$
I_{R_6}	$8I_m$	$3v_m$	$24v_m I_m$	I_{R_2}	-	-	-
I_{R_9}	$8.2I_m$	$2v_m$	$16.4v_m I_m$	I_{R_8}	$8.2I_m$	$2v_m$	$16.4v_m I_m$
I_{R_3}	-	-	-	I_{R_4}	-	-	-

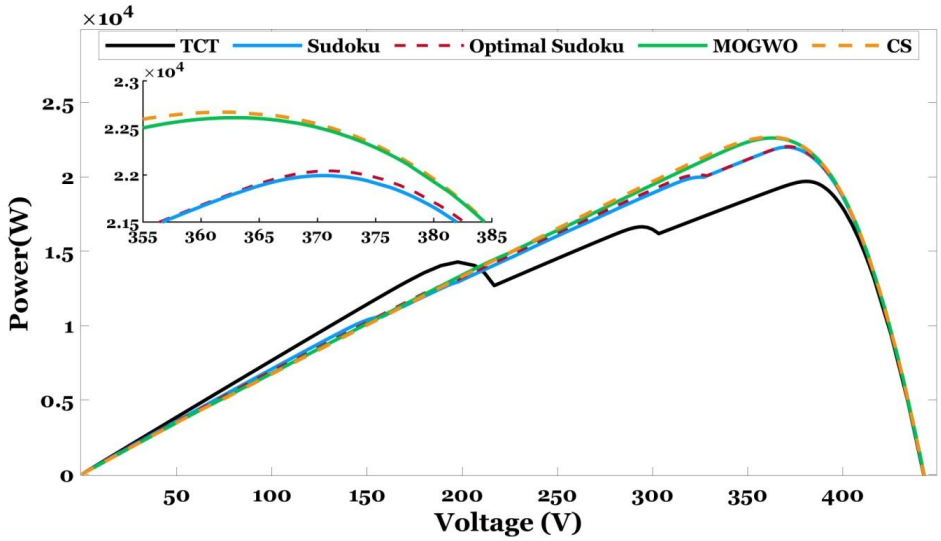

Figure 13. Characteristics of case 4 in terms of P-V.

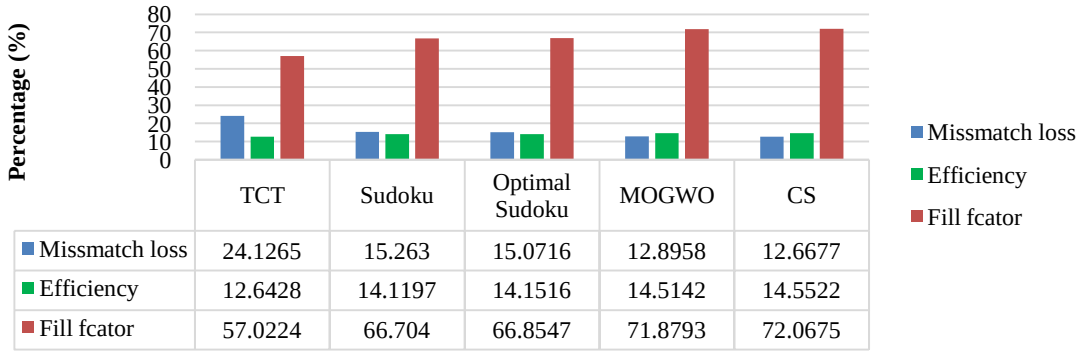

	TCT	Sudoku	Optimal Sudoku	MOGWO	CS
Missmatch loss	24.1265	15.263	15.0716	12.8958	12.6677
Efficiency	12.6428	14.1197	14.1516	14.5142	14.5522
Fill fcator	57.0224	66.704	66.8547	71.8793	72.0675

Figure 14. FF, ML, and efficiency for case 4.

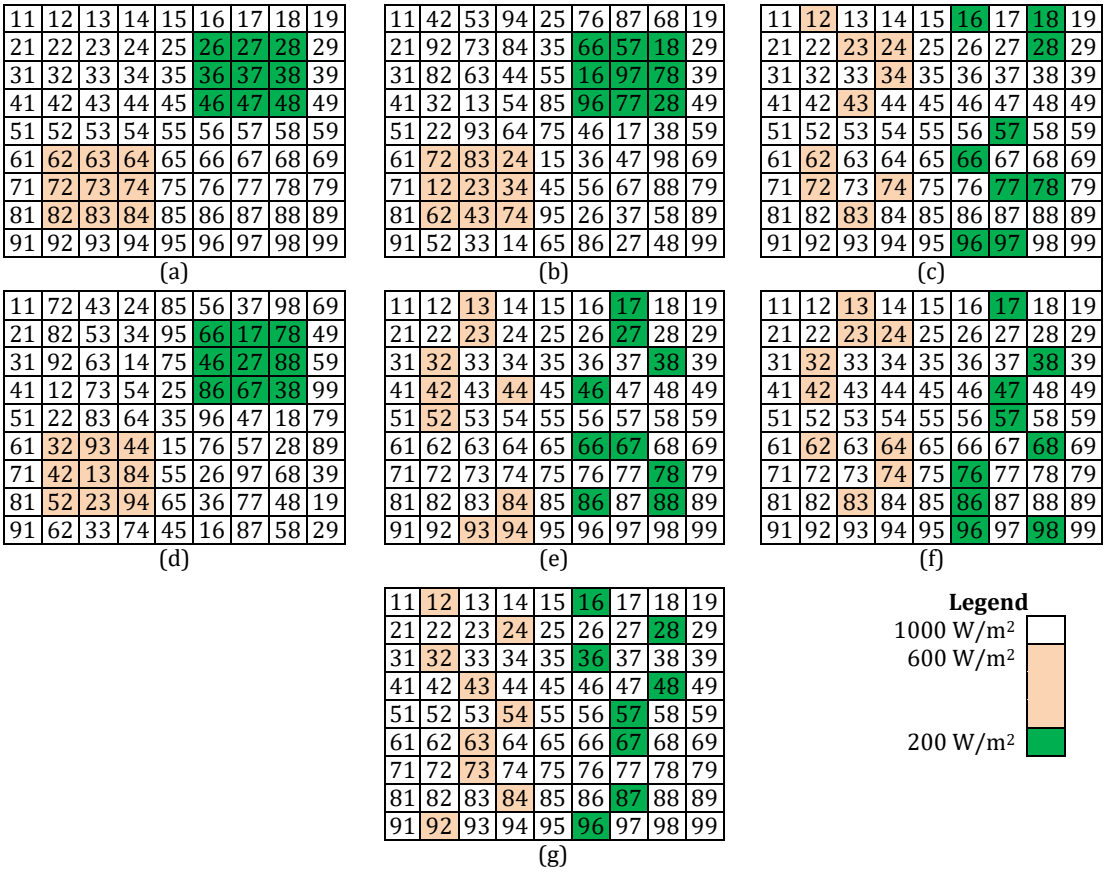

Figure 15. Results of case 5, (a) TCT scheme, (b) Sudoku arrangement, (c) Shade dispersion in Sudoku arrangement, (d) Optimal Sudoku arrangement, (e) Shade dispersion in Optimal Sudoku arrangement, (f) MOGWO, and (g) CS.

To assess the system's performance, current, voltage, and energy are evaluated in the same manner as in prior cases, and the results are displayed in Table 5. In this case, the suggested CS method produces more power (70.2 $v_m I_m$) than the other techniques. The simulation is used to evaluate the same, and the resulting P-V curve is shown in Figure 16. In this case, the proposed CS approach yields a greater power than MOGWO, Optimal sudoku, sudoku, and TCT, yielding 22.4937 kW, 22.2519 kW, 21.7446 kW, 20.9075 kW, and 20.5154 kW, respectively. The obtained parameters, such as ML (%), FF (%), and η (%) for all PV array topologies, are graphically displayed in Figure 17.

Table 5. Analysis of TCT, Sudoku, Optimal Sudoku, MOGWO, and CS schemes of case 5.

TCT				Sudoku				Optimal suduko			
I_{R_i}	$I(A)$	$V(V)$	$P(W)$	I_{R_i}	$I(A)$	$V(V)$	$P(W)$	I_{R_i}	$I(A)$	$V(V)$	$P(W)$
I_{R_4}	$6.6I_m$	$9v_m$	$59.4v_m I_m$	I_{R_7}	$6.6I_m$	$9v_m$	$59.4v_m I_m$	I_{R_8}	$7I_m$	$9v_m$	$63v_m I_m$
I_{R_3}	-	-	-	I_{R_1}	$7I_m$	$8v_m$	$56v_m I_m$	I_{R_6}	$7.4I_m$	$8v_m$	$59.2v_m I_m$
I_{R_2}	-	-	-	I_{R_9}	$7.4I_m$	$7v_m$	$51.8v_m I_m$	I_{R_4}	-	-	-
I_{R_8}	$7.8I_m$	$6v_m$	$46.8v_m I_m$	I_{R_2}	-	-	-	I_{R_3}	$7.8I_m$	$6v_m$	$46.8v_m I_m$
I_{R_7}	-		-	I_{R_6}	$7.8I_m$	$5v_m$	$39v_m I_m$	I_{R_2}	-	-	-
I_{R_6}	-	-	-	I_{R_5}	$8.2I_m$	$4v_m$	$32.8v_m I_m$	I_{R_1}	-	-	-
I_{R_9}	$9I_m$	$3v_m$	$27v_m I_m$	I_{R_8}	$8.6I_m$	$3v_m$	$25.8v_m I_m$	I_{R_9}	$8.2I_m$	$3v_m$	$24.6v_m I_m$
I_{R_5}	-	-	-	I_{R_4}	-	-	-	I_{R_7}	-	-	-
I_{R_1}	-	-	-	I_{R_3}	-	-	-	I_{R_5}	$8.6I_m$	$1v_m$	$8.6v_m I_m$

MOGWO				CS			
I_{R_i}	$I(A)$	$V(V)$	$P(W)$	I_{R_i}	$I(A)$	$V(V)$	$P(W)$
I_{R_9}	$7.4I_m$	$9v_m$	$66.6v_m I_m$	I_{R_9}	$7.8I_m$	$9v_m$	$70.2v_m I_m$
I_{R_6}	-	-	-	I_{R_8}	-	-	-
I_{R_8}	$7.8I_m$	$7v_m$	$54.6v_m I_m$	I_{R_7}	-	-	-
I_{R_7}	-	-	-	I_{R_6}	-	-	-
I_{R_4}	-	-	-	I_{R_5}	-	-	-
I_{R_3}	-	-	-	I_{R_4}	-	-	-
I_{R_1}	-	-	-	I_{R_3}	-	-	-
I_{R_5}	$8.2I_m$	$2v_m$	$16.4v_m I_m$	I_{R_2}	-	-	-
I_{R_2}	-	-	-	I_{R_1}	-	-	-

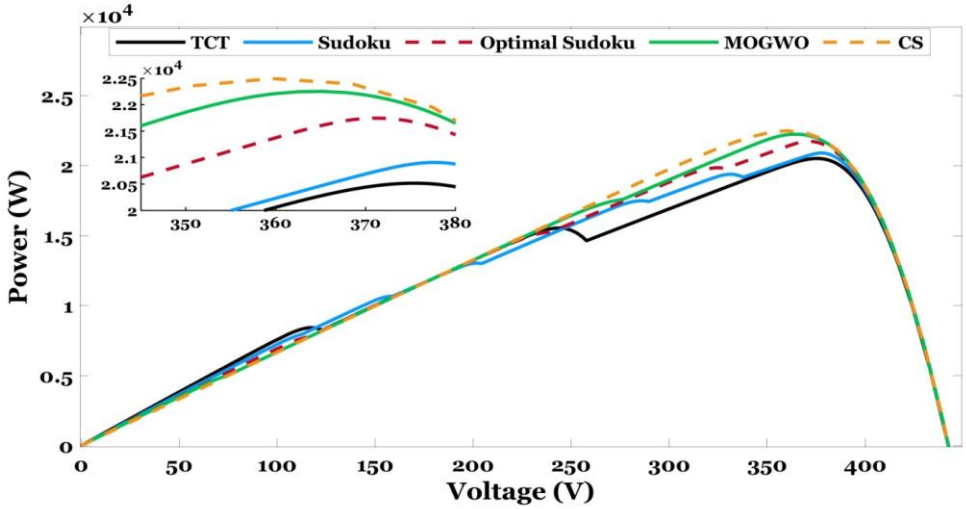

Figure 16. Characteristics of case 5 in terms of P-V.

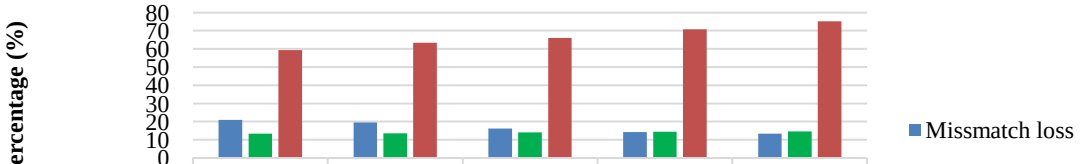

	TCT	Sudoku	Optimal Sudoku	MOGWO	CS
Missmatch loss	20.9572	19.4464	16.2212	14.2667	13.3351
Efficiency	13.321	13.5756	14.1191	14.4485	14.6055
Fill fcator	59.412	63.3595	65.9498	70.748	75.1464

Figure 17. FF, ML, and efficiency for case 5.

4. Conclusions

In this study, we introduce a novel approach for determining the optimal switching matrix configuration in partially shaded PV arrays using the CS optimization algorithm. The proposed method effectively mitigates mismatch losses by dynamically redistributing shaded modules, thereby enhancing overall system performance. Simulation results, conducted in MATLAB/Simulink on a 9 × 9 PV array subjected to five distinct shading patterns, demonstrate that the CS-based configuration consistently outperforms conventional methods, including TCT, standard Sudoku, Optimal Sudoku, and MOGWO. Quantitatively, the CS method achieves GMPP values of 23.6071 kW, 23.0057 kW, 22.1083 kW, 22.6669 kW, and 22.4937 kW across the tested shading scenarios, which represents an improvement of up to 8.7% over the best-performing alternative methods. Moreover, the CS configuration exhibits better FF, improved ML, and higher efficiency (η), demonstrating its robustness in resolving the multi-peak issue in the P–V characteristic curves. However, the current implementation assumes static environmental conditions and ideal switching behavior. The primary limitation lies in the absence of hardware-level validation and real-time control, which may introduce practical challenges such as switching delays, thermal effects, and increased system complexity. In the future, researchers should aim to integrate this optimization approach into real-time embedded systems, validate it through hardware-in-the-loop (HIL) simulations or physical prototypes, and explore its scalability to larger PV arrays. Additionally, combining CS with hybrid metaheuristic frameworks may yield further improvements in convergence speed and global search accuracy under rapidly changing environmental conditions.

Author contributions

Hassan S. Ahmed: Conceptualization, Methodology, Data curation, Formal analysis, Writing – original draft; Ahmed J. Abid: Supervision, Methodology, Data curation, Software, Validation, Writing – review & editing; Adel A. Obed: Supervision, Visualization, Project administration, Writing – review & editing; Raaid Alubady: Methodology, Resources, Writing – review & editing; Salam J. Yaqoob: Software, Data curation, Validation, Writing – review & editing; Ameer L. Saleh: Conceptualization, Methodology, Funding acquisition, Writing – review & editing; László Szabó: Project administration, Supervision, Writing – review & editing.

Use of Generative-AI tools declaration

The authors declare they have not used Artificial Intelligence (AI) tools in the creation of this article.

Conflict of interest

The authors declare there is no conflict of interest in this paper.

References

1. Taghvaee MH, Radzi MA, Moosavain SM, Hizam H, Marhaban MH (2013) A current and future study on non-isolated DC–DC converters for photovoltaic applications. *Renewable and sustainable energy reviews* 17: 216–227. https://doi.org/10.1016/j.rser.2012.09.023
2. Buberger J, Kersten A, Kuder M, Eckerle R, Weyh T, Thiringer T (2022) Total CO2-equivalent life-cycle emissions from commercially available passenger cars. *Renewable and Sustainable Energy Reviews* 159: 112158. https://doi.org/10.1016/j.rser.2022.112158
3. Abbas FA, Abdul-Jabbar TA, Obed AA, Kersten A, Kuder M, Weyh T (2023) A comprehensive review and analytical comparison of non-isolated dc-dc converters for fuel cell applications. *Energies* 16: 3493. https://doi.org/10.3390/en16083493
4. Sahoo SK (2016) Renewable and sustainable energy reviews solar photovoltaic energy progress in India: A review. *Renewable and Sustainable Energy Reviews* 59: 927–939. https://doi.org/10.1016/j.rser.2016.01.049
5. Yousri D, Allam D, Eteiba MB (2020) Optimal photovoltaic array reconfiguration for alleviating the partial shading influence based on a modified harris hawks optimizer. *Energy Conversion and Management* 206: 112470. https://doi.org/10.1016/j.enconman.2020.112470
6. Krishna GS, Moger T (2019) Improved SuDoKu reconfiguration technique for total-cross-tied PV array to enhance maximum power under partial shading conditions. *Renewable and Sustainable Energy Reviews* 109: 333–348. https://doi.org/10.1016/j.rser.2019.04.037
7. Pal P (2023) Present status and future outlooks of renewable energy in India for sustainable development. *A Basic Overview of Environment and Sustainable Development [Volume 2], International Academic Publishing House (IAPH),* 408–433. https://doi.org/10.52756/boesd.2023.e02.028
8. Villa LFL, Picault D, Raison B, Bacha S, Labonne A (2012) Maximizing the power output of partially shaded photovoltaic plants through optimization of the interconnections among its modules. *IEEE Journal of Photovoltaics* 2: 154–163. https://doi.org/10.1109/JPHOTOV.2012.2185040
9. Yaqoob SJ, Saleh AL, Motahhir S, Agyekum EB, Nayyar A, Qureshi B (2021) Comparative study with practical validation of photovoltaic monocrystalline module for single and double diode models. *Scientific reports* 11: 19153. https://doi.org/10.1038/s41598-021-98593-6
10. Rani BI, Ilango GS, Nagamani C (2013) Enhanced power generation from PV array under partial shading conditions by shade dispersion using Su Do Ku configuration. *IEEE Transactions on sustainable energy* 4: 594–601. https://doi.org/10.1109/TSTE.2012.2230033
11. Rao PS, Ilango GS, Nagamani C (2014) Maximum power from PV arrays using a fixed configuration under different shading conditions. *IEEE journal of Photovoltaics* 4: 679–686. https://doi.org/10.1109/JPHOTOV.2014.2300239

12. Sahu HS, Nayak SK, Mishra S (2015) Maximizing the power generation of a partially shaded PV array. *IEEE journal of emerging and selected topics in power electronics* 4: 626–637. https://doi.org/10.1109/JESTPE.2015.2498282
13. Alahmad M, Chaaban MA, kit Lau S, Shi J, Neal J (2012) An adaptive utility interactive photovoltaic system based on a flexible switch matrix to optimize performance in real-time. *Solar energy* 86: 951–963. https://doi.org/10.1016/j.solener.2011.12.028
14. Vicente PdS, Pimenta TC, Ribeiro ER (2015) Photovoltaic array reconfiguration strategy for maximization of energy production. *International Journal of Photoenergy* 2015: 592383. https://doi.org/10.1155/2015/592383
15. Satpathy PR, Sharma R (2019) Power and mismatch losses mitigation by a fixed electrical reconfiguration technique for partially shaded photovoltaic arrays. *Energy conversion and management* 192: 52–70. https://doi.org/10.1016/j.enconman.2019.04.039
16. Deshkar SN, Dhale SB, Mukherjee JS, Babu TS, Rajasekar N (2015) Solar PV array reconfiguration under partial shading conditions for maximum power extraction using genetic algorithm. *Renewable and Sustainable Energy Reviews* 43: 102–110. https://doi.org/10.1016/j.rser.2014.10.098
17. Babu TS, Ram JP, Dragičević T, Miyatake M, Blaabjerg F, Rajasekar N (2017) Particle swarm optimization based solar PV array reconfiguration of the maximum power extraction under partial shading conditions. *IEEE Transactions on Sustainable Energy* 9: 74–85. https://doi.org/10.1109/TSTE.2017.2714905
18. Horoufiany M, Ghandehari R (2018) Optimization of the Sudoku based reconfiguration technique for PV arrays power enhancement under mutual shading conditions. *Solar Energy* 159: 1037–1046. https://doi.org/10.1016/j.solener.2017.05.059
19. Akrami M, Pourhossein K (2018) A novel reconfiguration procedure to extract maximum power from partially-shaded photovoltaic arrays. *Solar Energy* 173: 110–119. https://doi.org/10.1016/j.solener.2018.06.067
20. Fathy A (2018) Recent meta-heuristic grasshopper optimization algorithm for optimal reconfiguration of partially shaded PV array. *Solar Energy* 171: 638–651. https://doi.org/10.1016/j.solener.2018.07.014
21. Yousri D, Babu TS, Beshr E, Eteiba MB, Allam D (2020) A robust strategy based on marine predators algorithm for large scale photovoltaic array reconfiguration to mitigate the partial shading effect on the performance of PV system. *IEEE Access* 8: 112407–112426. https://doi.org/10.1109/ACCESS.2020.3000420
22. Yousri D, Thanikanti SB, Balasubramanian K, Osama A, Fathy A (2020) Multi-objective grey wolf optimizer for optimal design of switching matrix for shaded PV array dynamic reconfiguration. *IEEE Access* 8: 159931–159946. https://doi.org/10.1109/ACCESS.2020.3018722
23. Mikkili S, Bapurao KA, Bonthagorla PK (2022) Sudoku and optimal sudoku reconfiguration techniques for power enhancement of partial shaded solar PV system. *Journal of The Institution of Engineers (India): Series B* 103: 1793–1807. https://doi.org/10.1007/s40031-022-00760-4
24. Rezazadeh S, Moradzadeh A, Pourhossein K, Akrami M, Mohammadi-Ivatloo B, Anvari-Moghaddam A (2023) Photovoltaic array reconfiguration under partial shading conditions for maximum power extraction via knight's tour technique. *Journal of Ambient Intelligence and Humanized Computing* 14: 11545–11567. https://doi.org/10.1007/s12652-022-03723-1
25. Fang X, Yang Q (2024) Dynamic reconfiguration of photovoltaic array for minimizing mismatch loss. *Renewable and Sustainable Energy Reviews* 191: 114160.

https://doi.org/10.1016/j.rser.2023.114160
26. Yi L, Cheng S, Wang Y, Ma H, Luo B, Hu Y (2024) A multi-objective pelican optimization algorithm for dynamic reconfiguration of multi-type rural rooftop PV array. *Journal of Intelligent & Fuzzy Systems* 47: 393–409. doi: https://doi.org/10.3233/JIFS-236528
27. Sharma M, Pareek S, Singh K (2024) An efficient power extraction using artificial intelligence based machine learning model for SPV array reconfiguration in solar industries. *Engineering Applications of Artificial Intelligence* 129: 107516. https://doi.org/10.1016/j.engappai.2023.107516
28. Hachemi AT, Sadaoui F, Saim A, Ebeed M, Arif S (2024) Dynamic operation of distribution grids with the integration of photovoltaic systems and distribution static compensators considering network reconfiguration. *Energy Reports* 12: 1623–1637. https://doi.org/10.1016/j.egyr.2024.07.050
29. Yi L, Cheng S, Wang Y, Hu Y, Ma H, Luo B (2024) A multivariate reconfiguration method for rooftop PV array based on improved northern goshawk optimization algorithm. *Physica Scripta* 99: 035537. https://doi.org/10.1088/1402-4896/ad2a2b
30. Khalil IU, ul Haq A (2024) A modified chess knight reconfiguration approach for mitigating power losses in PV systems. *Energy Reports* 11: 2204–2219. https://doi.org/10.1016/j.egyr.2024.01.066
31. Mallick P, Sharma R, Satpathy PR, Thanikanti SB, Nwulu NI (2024) A harmony search switching matrix algorithm for enhanced performance of solar PV arrays during non-uniform irradiance scenarios. *IEEE Access* 12: 40387–40411. https://doi.org/10.1109/ACCESS.2024.3370839
32. Hou G, Guo Z (2025) Maximum power point tracking of solar photovoltaic under partial shading conditions based on improved salp swarm algorithm. *Electric Power Systems Research* 241: 111316. doi: https://doi.org/10.1016/j.epsr.2024.111316
33. Azharuddin M, Babu TS, Bilakanti N, Rajasekar N (2016) A nearly accurate solar photovoltaic emulator using a dSPACE controller for real-time control. *Electric Power Components and Systems* 44: 774–782. https://doi.org/10.1080/15325008.2015.1131763
34. Babu TS, Ram JP, Sangeetha K, Laudani A, Rajasekar N (2016) Parameter extraction of two diode solar PV model using Fireworks algorithm. *Solar energy* 140: 265–276. https://doi.org/10.1016/j.solener.2016.10.044
35. Yousri D, Allam D, Eteiba MB, Suganthan PN (2019) Static and dynamic photovoltaic models' parameters identification using chaotic heterogeneous comprehensive learning particle swarm optimizer variants. *Energy conversion and management* 182: 546–563. https://doi.org/10.1016/j.enconman.2018.12.022
36. Allam D, Yousri D, Eteiba M (2016) Parameters extraction of the three diode model for the multi-crystalline solar cell/module using Moth-Flame Optimization Algorithm. *Energy Conversion and Management* 123: 535–548. https://doi.org/10.1016/j.enconman.2016.06.052
37. Yang XS, Deb S (2009) Cuckoo search via Lévy flights. In *2009 World congress on nature & biologically inspired computing (NaBIC)*, 210–214. Ieee. https://doi.org/10.1109/NABIC.2009.5393690

AIMS Press